THE JOURNAL OF BIOLOGICAL CHEMISTRY VOL. 285, NO. 36, pp. 27652–27663, September 3, 2010

A Novel Glycerophosphodiester Phosphodiesterase, GDE5, Controls Skeletal Muscle Development via a Non-enzymatic Mechanism*[S]

Received for publication, January 21, 2010, and in revised form, June 8, 2010 Published, JBC Papers in Press, June 24, 2010, DOI 10.1074/jbc.M110.106708

Yuri Okazaki[‡1], Noriyasu Ohshima[§1], Ikumi Yoshizawa[‡1], Yasutomi Kamei[¶], Stefania Mariggiò[‖], Keiko Okamoto[‡], Masahiro Maeda[‡], Yoshihito Nogusa[‡], Yuichiro Fujioka[‡], Takashi Izumi[§], Yoshihiro Ogawa[¶], Yoshitsugu Shiro[‡‡], Masanobu Wada[§§], Norihisa Kato[‡], Daniela Corda[‖**], and Noriyuki Yanaka[‡2]**

*From the [‡]Department of Molecular and Applied Bioscience, Graduate School of Biosphere Science, Hiroshima University, Higashi-Hiroshima 739-8528, Japan, the [§]Department of Biochemistry, Gunma University Graduate School of Medicine, Gunma 371-8511, Japan, the [¶]Department of Molecular Medicine and Metabolism, Medical Research Institute, Tokyo Medical and Dental University, Tokyo 113-8510, Japan, the [‖]Department of Cell Biology and Oncology, Consorzio Mario Negri Sud, Santa Maria Imbaro, 66030 Chieti, Italy, the **Institute of Protein Biochemistry, National Research Council, 80131 Naples, Italy, the [‡‡]RIKEN SPring-8 Center, Harima Institute, Hongo 679-5148, Japan, and the [§§]Department of Human Sciences, Graduate School of Integrated Arts and Sciences, Hiroshima University, Higashi-Hiroshima 739-8521, Japan*

Mammalian glycerophosphodiester phosphodiesterases (GP-PDEs) have been identified recently and shown to be implicated in several physiological functions. This study isolated a novel GP-PDE, GDE5, and showed that GDE5 selectively hydrolyzes glycerophosphocholine (GroPCho) and controls skeletal muscle development. We show that GDE5 expression was reduced in atrophied skeletal muscles in mice and that decreasing GDE5 abundance promoted myoblastic differentiation, suggesting that decreased GDE5 expression has a counter-regulatory effect on the progression of skeletal muscle atrophy. Forced expression of full-length GDE5 in cultured myoblasts suppressed myogenic differentiation. Unexpectedly, a truncated GDE5 construct (GDE5ΔC471), which contained a GP-PDE sequence identified in other GP-PDEs but lacked GroPCho phosphodiesterase activity, showed a similar inhibitory effect. Furthermore, transgenic mice specifically expressing GDE5ΔC471 in skeletal muscle showed less skeletal muscle mass, especially type II fiber-rich muscle. These results indicate that GDE5 negatively regulates skeletal muscle development even without GroPCho phosphodiesterase activity, providing novel insight into the biological significance of mammalian GP-PDE function in a non-enzymatic mechanism.

The mass and composition of skeletal muscle are closely associated with its physiological functions, such as exercise, energy expenditure, and glucose metabolism (1, 2). Progressive muscle loss, frequently caused by diabetes, obesity, and decreased physical activity (sarcopenia), is a major health problem in our aging society (3). In the search for clues as to the regulation of skeletal muscle mass and composition during physical exercise and muscular atrophy caused by disease and disuse, a number of metabolites have been investigated in adult skeletal muscles. In human and mouse skeletal muscle tissues, deacylated glycerophospholipids, the glycerophosphodiesters (GPs),[3] were analyzed as phosphate-containing compounds, and interestingly, the amounts of skeletal muscle GPs are reportedly altered in response to physical activity, the environment, and pathological conditions (4–6). However, the biological functions of skeletal muscle GPs and the physiological regulation of their levels have not been studied to date.

The GPs (primarily glycerophosphoinositol and glycerophosphocholine) are cellular products of phospholipase activities on membrane phospholipids. GP intracellular concentrations vary with oncogenic transformation, cell differentiation, and environmental stimuli, and they are thought to be tightly controlled for the balance between synthesis and degradation (7–9). For GP hydrolysis, two bacterial enzymes have been isolated and studied in depth at the molecular level. Glycerophosphodiester phosphodiesterases (GP-PDEs), GlpQ and UgpQ, were identified as periplasmic and cytosolic proteins that have essential roles in the hydrolysis of GPs to glycerol 3-phosphate and alcohol, which are used as major sources of carbon and phosphate (10, 11). In contrast, three mammalian GP-PDEs, GDE1, GDE2, and GDE3, were previously identified and presumed to have distinct physiological functions (12–15). In initial studies, GDE1 (also known as MIR16) was isolated as a unique membrane protein that interacted with RGS16, a regulator of G-protein signaling (12), and it has been shown to preferentially hydrolyze glycerophosphoinositol (GroPIns) in response to β-adrenergic stimulation (16). Studies on GDE2 show that retinoic acid-induced expression of GDE2 has critical roles in neuronal differentiation and neurite outgrowth of motor neurons (15, 17). Furthermore, it is reported that GDE3 is regulated during osteoblast development and induces osteo-

* This work was supported in part by a grant-in-aid for scientific research from the Ministry of Education, Culture, Sports, Science, and Technology of Japan. This work was also supported by Telethon Italia.

[S] The on-line version of this article (available at http://www.jbc.org) contains supplemental "Methods," Figs. S1–S4, and Table S1.

[1] These authors contributed equally to this work.

[2] To whom correspondence should be addressed. Tel.: 81-82-4247979; Fax: 81-82-4247916; E-mail: yanaka@hiroshima-u.ac.jp.

[3] The abbreviations used are: GP, glycerophosphodiester; GP-PDE, glycerophosphodiester phosphodiesterase; GroPIns, glycerophosphoinositol; GroPCho, glycerophosphocholine; EST, expressed sequence tag; G3P, glycerol 3-phosphate; MBP, maltose-binding protein.

blast differentiation and morphological changes in cultured mammalian cells (13). In addition, our recent study demonstrates that GDE3 is a GroPIns phosphodiesterase that hydrolyzes GroPIns to glycerol and inositol 1-phosphate, unlike the bacterial GP-PDEs and GDE1 (18). In mammalian cells, GroPIns is being increasingly recognized as an important intracellular messenger that is involved in various cellular signaling pathways such as cell proliferation, transformation, and differentiation (9, 18, 19). Although these observations strongly suggest a central role of mammalian GP-PDEs in regulating intracellular GP concentrations, previous reports on the existence of proteins that interact with mammalian GP-PDEs, such as RGS16, PRAF2 (also known as JM4), and Prdx1 (12, 20, 21), have prompted us to consider that GP-PDEs might also act via a non-enzymatic mechanism. Thus, mammalian GP-PDEs are most likely involved in a variety of cellular events (22). However, at the molecular level, their potential roles remain unclear, including the control of intracellular GP levels and other possible unknown effects.

As the characterization of these unidentified GP-PDEs will be highly informative for understanding their molecular basis, we explored novel mammalian GP-PDE cDNAs using sections of the GP-PDE sequence to locate expressed sequence tags (ESTs). For this study, we focused on a cDNA termed GDE5, showing that GDE5 is a novel glycerophosphocholine (GroPCho) phosphodiesterase and also that GDE5 has an inhibitory role in skeletal muscle differentiation that is carried out independently of its GroPCho enzymatic activity.

EXPERIMENTAL PROCEDURES

Materials—Restriction endonucleases and DNA-modifying enzymes were purchased from TaKaRa Bio (Kyoto, Japan). HEK293T cells, mouse C2C12 myoblasts, and rat L6 skeletal cells were obtained from the Health Science Research Resources Bank (Sennan, Japan). Dulbecco's modified Eagle's medium (DMEM) and fetal calf serum (FCS) were purchased from Invitrogen. Glycerophosphocholine, phosphatidylserine, phosphatidylethanolamine, phosphatidylglycerol, phosphatidylinositol, β-nicotinamide adenine dinucleotide (NAD), and *sn*-glycerol-3-phosphate dehydrogenase were from Sigma. PCR primers were purchased from Operon Biotechnologies (Tokyo).

Isolation of GDE5—An amino acid sequence (residues 500–875) containing a putative GP-PDE domain of human GDE3 was used as a query to search a database of ESTs with BLAST (basic local alignment search tool). Many EST sequences showing homology to the query sequence were obtained, and we examined whether these might encode a known or a novel GP-PDE by searching the GenBank™ database with BLAST.

Expression and Purification of Recombinant Mouse GDE5 in Insect Cells—The cDNA encoding mouse GDE5 was obtained from FANTOM2 clones (clone ID: 5430401O18) (23) and subcloned into pENTER™/D-TOPO (Invitrogen). The cDNA was inserted into BaculoDirect™ C-Term linear DNA, which added the V5 peptide and a His_6 tag at the C terminus of GDE5. Sf9 cells (Invitrogen) were transfected with the DNA using Cellfectin (Invitrogen) to produce the baculovirus. Sf9 cells were cultured in Sf-900II SFM (Invitrogen) containing 10% Grace's insect medium (Invitrogen), 1% FCS, 1 μg/ml gentamicin (Invitrogen), 0.25 μg/ml amphotericin B, and 0.2% pluronic (Sigma). For large-scale production of GDE5, Sf9 cells were transfected with the baculovirus at a minimum multiplicity of infection of 2. The cells were collected by centrifugation 48 h after transfection. The cells were disrupted by sonication in 20 mM Tris-HCl, pH 8.0, 500 mM NaCl. The cell debris was removed by centrifugation at 800 × *g* for 10 min at 4 °C. The supernatant was further centrifuged at 100,000 × *g* for 60 min at 4 °C. The supernatant was subjected to a Ni^{2+}-bound HiTrap chelating column (GE Healthcare) equilibrated with 20 mM Tris-HCl, pH 8.0, containing 500 mM NaCl and 50 mM imidazole. The protein was eluted with the same buffer without the 500 mM imidazole. The eluate was desalted and then subjected to a Resource Q column (GE Healthcare) equilibrated with 20 mM Tris-HCl, pH 8.0. GDE5 was eluted with a linear gradient of NaCl. The GDE5-containing fractions were then applied to a HiLoad 16/60 Superdex 200 column (GE Healthcare) equilibrated with 20 mM Tris-HCl, pH 8.0, 200 mM NaCl.

GDE Assay—Cd^{2+}-free GroPCho was prepared as described previously (24). The other glycerophosphodiesters were prepared from their phospholipid precursors (25). GDE activity was examined using an enzyme-coupled spectrophotometric assay, measuring the amount of glycerol 3-phosphate (G3P) generated by the enzyme reaction. The reaction mixture contained the following: 50 mM HEPES-NaOH, pH 7.4, 10 mM $MgCl_2$, 0.5 mM glycerophosphodiesters, and 5 μg/ml GDE5. The reaction mixture was incubated at 37 °C. The reaction was stopped by adding EDTA to a final concentration of 20 mM. The amount of G3P produced by the GDE5 activity was measured separately using G3P dehydrogenase. The assay mixture contained 0.2 M hydrazine-glycine buffer, pH 9.0, 1 mM NAD, 10 units/ml G3P dehydrogenase, and the GDE5 reaction mixture to a final volume of 200 μl. The assay mixture was incubated at 37 °C for 1 h until oxidation of G3P by the G3P dehydrogenase was complete. The G3P concentration was calculated from the absorbance change at 340 nm. Kinetic data were analyzed using Enzyme Kinetics Pro software (ChemSW Inc., Fairfield, CA).

Cell Cultures and Transfection—HEK293T, C2C12, and L6 cells were cultured in DMEM supplemented with 10% FCS, 100 units/ml penicillin, and 100 μg/ml streptomycin under a humidified atmosphere of 5% CO_2 in air at 37 °C. For studies examining the sequence of myoblast differentiation, the cells were seeded at 5000 cells/cm^2 in 24-well plates. After these cells reached confluence (day 0), the medium was replaced with myogenic medium, consisting of DMEM supplemented with 2% horse serum. The medium was replaced every 2 days. A cDNA encoding full-length mouse GDE5 was subcloned into the SalI (made blunt with T4 DNA polymerase) and NotI sites of the mammalian expression vector pEF/myc/cyto (Invitrogen), generating pEF-GDE5. To obtain a deletion mutant of GDE5 (amino acids 1–470, GDE5ΔC471), cDNA was applied using a PCR primer set (5′-GGGGATCCTATCCATCCCTGTGTTGGCAAA-3′ and 5′-GCGCGGCCCGGACCGGCAGAAATCC-3′) designed according to the nucleotide sequences of mouse GDE5 and subcloned into pEF/myc/cyto, which generated pEF-GDE5ΔC471. DNA transfections were performed

using Lipofectamine 2000 (Invitrogen) according to the manufacturer's instructions. Stealth siRNA duplex oligoribonucleotides against mouse GDE5 were synthesized by Invitrogen. The sequences were as follows: sense, 5′-CAGUGUGUUGUGGAAAGCAGUGAUU-3′; antisense, 5′-AAUCACUGCUUUCCACAACACACUG-3′. C2C12 cells were transfected with these siRNAs to a final concentration of 20 nM using Lipofectamine RNAimax (Invitrogen). For retroviral expression, cDNAs encoding mouse GDE5 and GDE5ΔC471 were subcloned into the pLXSN retrovirus vector (Clontech, Palo Alto, CA). High titer retroviruses harboring GDE5 were produced in Phoenix 293 cells and used to infect L6 cells as reported previously (Yanaka *et al.* (17)). After infection into L6 cells, these cells were treated with 500 μg/ml G418 for 7 days and used to evaluate myogenesis. For stable transfection of C2C12 cells, the cells were transfected with Lipofectamine 2000 using pEF-GDE5, pEF-GDE5ΔC471, or vector pEF/myc/cyto (control). After replating, these cells were treated with 500 μg/ml G418 for 14 days. G418-resistant colonies were identified and reseeded at 5000 cells/cm^2. After 2 days, the medium was replaced with myogeneic medium (day 0). At day 6, the morphology of each cell line was observed under light microscopy, and the C2C12 cells were fixed and subjected to immunofluorescent staining using mouse anti-myosin (fast) antibody (Sigma), which was visualized with fluorescein isothiocyanate- or Cy3-conjugated secondary antibodies (GE Healthcare).

Preparation of GDE5 Antibody and Western Blotting—A cDNA encoding part of the mouse GDE5 (amino acids 1–163) was subcloned into the maltose-binding protein (MBP) expression vector pMAL-c (New England Biolabs, Beverly, MA), generating pMAL-GDE5. The MBP fusion construct pMAL-GDE5 was introduced into the bacterial strain JM109 (Toyobo, Osaka, Japan). Preparation of the MBP-GDE5 fusion protein was performed as reported previously (13). A polyclonal antibody raised against GDE5 was obtained by injecting rabbits with MBP-GDE5 in Freund's complete adjuvant (Difco Laboratories Inc., Detroit, MI). The antibody was affinity-purified using an antigen-coupled Sepharose column (GE Healthcare) according to the manufacturer's instructions.

HEK293T and C2C12 cells were washed with ice-cold PBS and scraped into ice-cold radioimmune precipitation assay buffer (10 mM Tris-HCl, pH 7.4, 1% Nonidet P-40, 0.1% sodium deoxycholate, 0.1% SDS, 0.15 M NaCl, and 1 mM EDTA). The homogenates were centrifuged at 10,000 × *g* for 10 min. Protein concentrations of the supernatants were determined using a Bio-Rad protein assay kit (Bio-Rad). Ten micrograms (protein equivalents) of the supernatant were subjected to SDS-PAGE and transferred to Immobilon P filters (Millipore, Bedford, MA). The filters were blocked for 18 h at 4 °C by soaking in 4% nonfat dried milk (Nacalai Tesque, Kyoto, Japan) in PBS; then they were incubated for 18 h at 4 °C with the anti-GDE5 antibody (diluted 1:1000). The signals were detected using horseradish peroxidase-conjugated anti-rabbit IgG and the enhanced chemiluminescence system (GE Healthcare).

Northern Blotting—Total RNA was obtained from mouse tissues using the RNeasy kit (Qiagen Sciences, Germantown, MD) according to the manufacturer's instructions. Total RNAs were fractionated in 1% agarose gels containing 0.66 M formaldehyde and 0.02 M MOPS (pH 7.0). The fractionated RNAs were transferred onto nylon filters by capillary blotting and then cross-linked by ultraviolet irradiation. ^{32}P-Labeled cDNA fragments encoding mouse GDE5, mouse troponin I (type II), mouse troponin C (type II), human glyceraldehyde-3-phosphate dehydrogenase (GAPDH), and human β-actin were used as probes for northern blotting. Hybridization was performed in 6× SSC, 0.5% SDS, 5× Denhardt's solution, and 100 μg/ml salmon sperm DNA at 65 °C for 16 h with the probe. The membranes were washed with 0.1× SSC and 0.5% SDS at 65 °C for 1 h and exposed to imaging plates (Fuji Film, Tokyo).

Animals—C57BL/6 mice (Charles River Japan) were housed in a room with controlled temperature (24 °C) and a 12-h light/dark cycle (lights on, 8:00 a.m. to 8:00 p.m.). The animals were given free access to diet and deionized water. The mice were maintained according to the Guide for the Care and Use of Laboratory Animals established by Hiroshima University. The right hind limbs of the male mice were immobilized in plaster casts, and the left hind limbs were left freely moving for the control samples. After 3 weeks of immobilization in plaster casts, total RNA was isolated from the skeletal muscle (gastrocnemius) of the right and left hind limbs. Denervation of one gastrocnemius was carried out by removing a 1-cm section of sciatic nerve just beneath the biceps femoris muscle of the male mice at 9 weeks of age. After 3 days, the total RNA from the gastrocnemius was subjected to Northern blotting.

The human skeletal muscle α-actin promoter was provided by Drs. E. D. Hardeman and K. Guven (Children's Medical Research Institute, Westmead, Australia). The transgene construct contained from −2000 to +200 base pairs of the human α-skeletal actin promoter, 2.0 kb of complete mouse GDE5 cDNA, and a polyadenylation signal encoded by bovine growth hormone. The transgene was excised from agarose gel, purified, and used for microinjection into BDF1 mouse eggs at Japan SLC Inc. (Hamamatsu, Japan). Among 81 mouse pups, two lines, Tg7 and Tg31, were studied. The male chimeras harboring the GDE5 transgene were mated with C57BL/6J female mice to obtain F1 offspring. The heterozygous F1 male offspring from this breeding were then backcrossed with purebred C57BL/6J females to obtain F2 offspring; this process was continued until the F3 generation of mice was obtained. The male heterozygous GDE5 transgenic mice and their littermate wild-type mice were sacrificed at 10–14 weeks of age.

Blood Analysis—Food was withdrawn 6 h before decapitation. Blood was collected, and the plasma was immediately separated by centrifugation (10 min at 900 × *g*) and stored at −20 °C. Glucose, free fatty acids, and triglycerides were measured by Test Wako (Wako Biochemicals, Osaka, Japan) according to the manufacturer's instructions.

Histological Analysis—Samples of the skeletal muscle (gastrocnemius) of wild-type (WT) and GDE5ΔC471 mice at 14 weeks of age were frozen in liquid nitrogen-cooled isopentane (Sigma), and transverse serial sections were stained with hematoxylin and eosin (H&E).

DNA Microarray—Total RNA derived from the skeletal muscle (gastrocnemius) of WT and GDE5ΔC471 mice at 12 weeks of age was isolated using an RNeasy kit and RNase-Free DNase set (Qiagen) and subjected to cRNA synthesis for a DNA

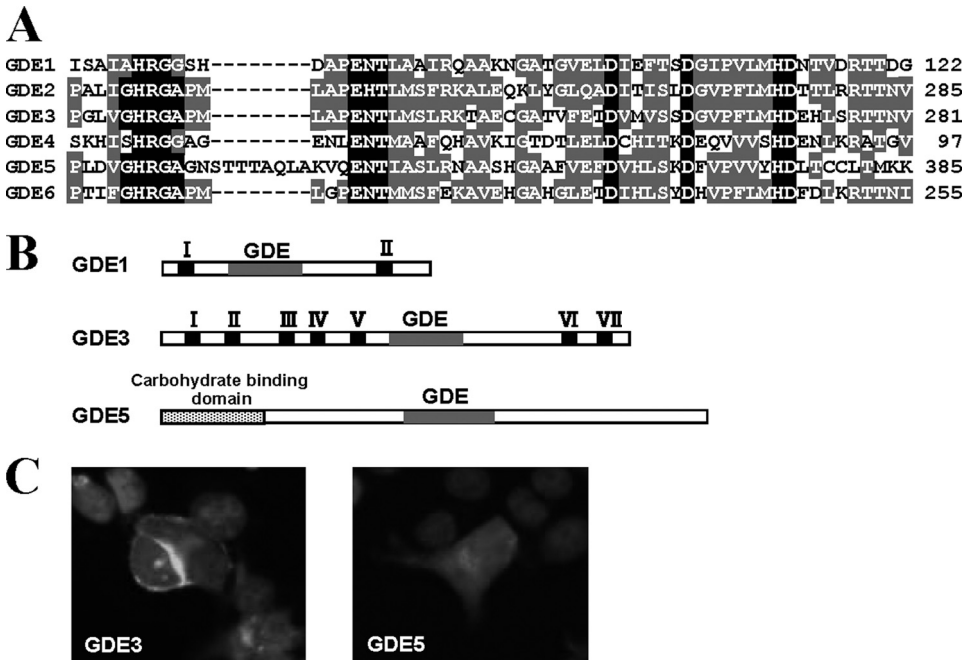

FIGURE 1. **GDE5 is a novel cytosolic glycerophosphodiester phosphodiesterase.** *A*, deduced amino acid sequences of the catalytic regions of mouse GP-PDEs. *Black boxes*, identical amino acids; *gray boxes*, similar amino acids. *B*, schematic diagram illustrating the domain structures of the three mouse GP-PDEs. Putative transmembrane domains are *numbered* from the N terminus. *GDE*, represents the putative GP-PDE domain. *C*, expression of GDE3 and GDE5 in HEK293T cells. HEK293T cells were transiently transfected with GFP-GDE3 (*GDE3*) or GFP-GDE5 (*GDE5*). GFP-GDE3 accumulated at the cell periphery, whereas GFP-GDE5 was localized in the cytoplasm.

microarray analysis according to the manufacturer's instructions (whole mouse genome 60-mer oligo microarray, Agilent Technologies, Palo Alto, CA). All of the procedures of fluorescence labeling, hybridization, and slide and image processing were carried out according to the manufacturer's instructions. Briefly, aliquots of cRNA samples were fragmented and hybridized on the whole mouse genome oligo microarray slides at 65 °C for 17 h. The slides were then sequentially washed, dried, and scanned using an Agilent DNA microarray scanner with SureScan technology (Agilent Technologies). In this study, the DyeSwap method was used to eliminate the bias between dyes. Gene expression data were obtained with Agilent Feature Extraction software, using defaults for all parameters except ratio terms, which were changed according to the Agilent protocol to fit the direct labeling procedure. Files and images, including error values and *p* values, were exported from Agilent Feature Extraction software (version 9.5).

RT-PCR Analyses—Semiquantitative and quantitative PCR analyses were performed on total RNA prepared with an RNeasy kit and RNase-Free DNase set (Qiagen). The reverse transcriptase reaction was carried out with 1 μg of total RNA as a template to synthesize cDNA using SuperScript II reverse transcriptase and random hexamers (Invitrogen) according to the manufacturer's instructions. For semiquantitative PCR analysis, cDNA and primers were added to the GoTaq Master Mix (Promega, Madison, WI) to give a total reaction volume of 20 μl. The reactions were sampled after 25, 28, and 30 cycles under different PCR conditions to monitor product accumulation. For quantitative PCR analysis, cDNA and primers were added to the Power SYBR Green PCR Master Mix (Applied Biosystems, Foster City, CA) to give a total reaction volume of 15 μl. PCR reactions were then performed using an iCycler thermocycler (Bio-Rad). Conditions were set to the following parameters: 10 min at 95 °C followed by 45 cycles each for 15 s at 95 °C and 1 min at 60, 62, or 64 °C. The primers used for real-time PCR analysis were as follows: GDE5, forward, 5′-TTTGATGTCCACCTTTCAAAGGAC-3′, and reverse, 5′-CTCCATCCCTGTGTTGGCAAATCC-3′; myogenin, forward, 5′-CATGTAAGGTGTGTAAGAGG-3′, and reverse, 5′-GCGAGCAAATGATCTCCTGG-3′; skeletal muscle creatine kinase, forward, 5′-GCGAGTTCAAGGGCAAATAC-3′, and reverse, 5′-TGTTGTCGTTGTGCCAGATG-3′; β-actin, forward, 5′-TTGGGTATGGAATCCTGTGGCATC-3′, and reverse, 5′-CGGACTCATCGTACTCCTGCTTGC-3′.

RESULTS

Isolation of a Novel Glycerophosphocholine Phosphodiesterase, GDE5—Using a bioinformatics approach, the nucleotide sequence corresponding to the GP-PDE domain of mouse GDE3 was used to search the EST database. The homologous sequences contained the GP-PDE motif (pfam03009), which was found in human and mouse cDNA libraries (human, NM_019593; mouse, NM_028802). The mouse cDNA, termed GDE5(16), was shown to encode a protein of 675 amino acids with a predicted molecular mass of 76,578 Da. On the basis of the amino acid sequence of GDE5, we predicted that the protein contains a putative catalytic domain that shares a common motif (amino acids 320–385, Fig. 1*A*) with other GP-PDEs. Interestingly, GDE5 does not have a transmembrane region, as seen for other mammalian GP-PDEs; instead, it has an N-terminal carbohydrate binding domain (Fig. 1*B*) that is often found in glycosylhydrolases, such as amylases. We observed that the GDE5 protein was localized in the cytoplasm, indicating that unlike other mammalian GP-PDEs, GDE5 can function as a cytosolic protein (Fig. 1*C*). As mentioned previously, recent reports have shown the remarkable characteristics of GroPIns as a water-soluble and bioactive intracellular derivative of phosphatidylinositol that is involved in a variety of cellular signaling pathways (9, 19). GDE1 and GDE3 can hydrolyze GroPIns (16, 18); however, the catalytic domain of these proteins is localized extracellularly and is enzymatically active in the extracellular space (13, 16). These observations raise the possibility that GDE5 is a candidate for the direct regulation of the intracellular GroPIns levels. However, enzymatic assays using postnuclear preparations of HEK293T cells transfected with pET-GDE5 or pET empty vector (supplemental Fig. S1*A*) indicated that GDE5 cannot hydrolyze GroPIns or GroPIns4P (data not shown). In addition, CHO cells

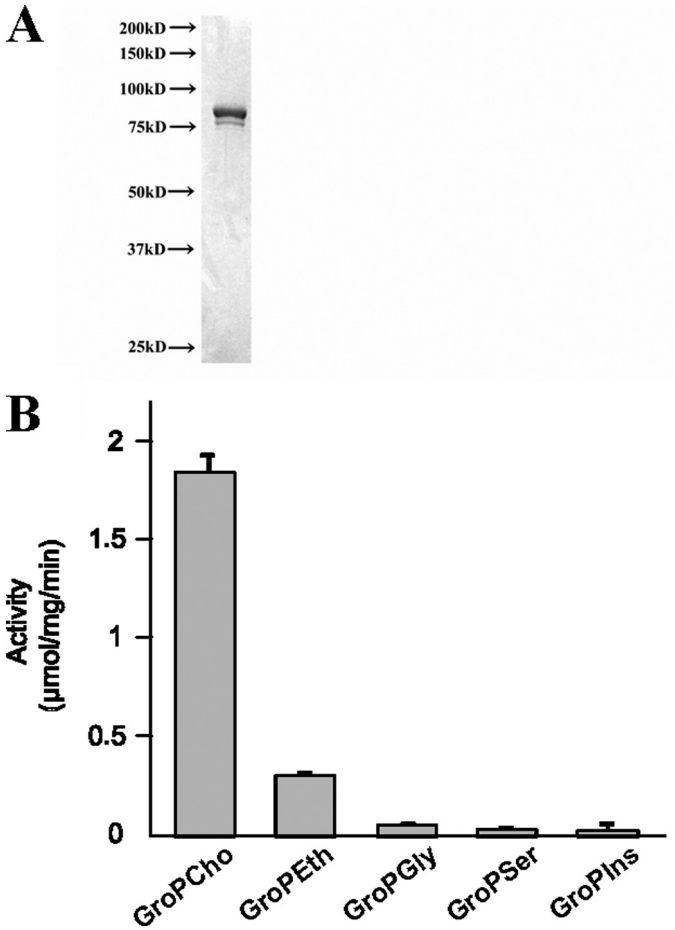

FIGURE 2. **GDE5 is a glycerophosphocholine phosphodiesterase.** *A*, His-tagged mouse GDE5 protein was overexpressed in baculovirus-infected Sf9 insect cells. Mouse recombinant GDE5 was purified as determined by SDS-PAGE. A single protein band was detected at 81 kDa, which corresponded to the calculated molecular mass of His-tagged mouse GDE5. *B*, substrate specificity of mouse GDE5. GDE activity was examined by an enzyme-coupled spectrophotometric assay. The substrates used were GroPCho, glycerophosphoethanolamine (*GroPEth*), glycerophosphoglycerol (*GroPGly*), glycerophosphoserine (*GroPSer*), and GroPIns. The data are from a single experiment carried out in triplicate (mean ± S.D.) and are representative of two independent experiments.

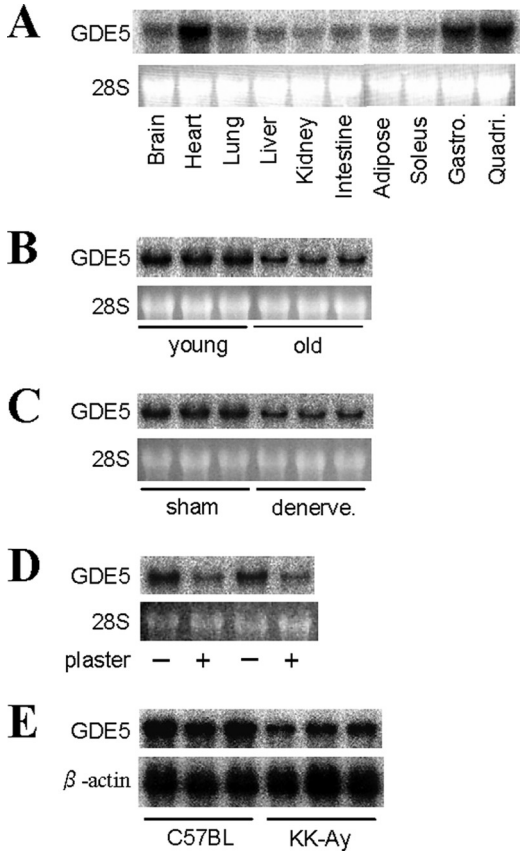

FIGURE 3. **GDE5 mRNA expression in skeletal muscle.** *A*, GDE5 mRNA was highly expressed in mouse muscle tissues. A mouse multiple tissue Northern blot with 20 μg of total RNAs was probed with GDE5 cDNA. *B*, 20 μg of total RNA from the gastrocnemius of male mice at 5 months (*young*) and 27 months (*old*) of age was subjected to Northern blotting. *C*, denervation (*denerve.*) of one gastrocnemius was carried out by removing the sciatic nerve of male mice at 9 weeks of age. After 3 days, total RNA (15 μg/lane) from the gastrocnemius of sham-operated (*sham*) and denervation mice was subjected to Northern blotting. *D*, after immobilization in plaster casts, Northern blotting was performed on total RNA (20 μg/lane) isolated from the gastrocnemius of the right and left hind limbs. *E*, 10 μg of total RNA from the gastrocnemius of male C57BL and KK-Ay mice was subjected to Northern blotting.

transfected with pET-GDE5 and pET empty vector showed either the same basal (1392.2 ± 173.6 and 1392.7 ± 13 cpm, respectively) and ATP-stimulated (about 1.3-fold basal) intracellular GroPIns levels (supplemental Fig. S1, *A* and *B*). These data strongly suggest that GroPIns is not a GDE5 substrate. To characterize the substrate specificity for GDE5, we overexpressed a His-tagged GDE5 in insect Sf9 cells. Mouse recombinant GDE5 was purified to near homogeneity from baculovirus-infected Sf9 cells, as determined by SDS-PAGE. A single protein band was observed at 81 kDa (Fig. 2*A*), which corresponded to the calculated molecular mass of His-tagged GDE5. Several types of GPs were tested as substrates for the purified GDE5 in the presence of Mg^{2+}. The specific activities of purified GDE5 toward GroPCho and glycerophosphoethanolamine were 2.0 ± 0.09 and 0.34 ± 0.03 μmol/mg/min, respectively (Fig. 2*B* and supplemental Fig. S2). There was no significant reactions when glycerophosphoglycerol, GroPIns, and glycerophosphoserine were used as substrates (Fig. 2*B*), showing that GDE5 has a marked substrate preference for GroPCho. Because GP-PDEs were previously shown to be affected by bivalent metal ions (24), we tested the effects of Ca^{2+} on GDE5 activity, which is most effective for bacterial GlpQ. We could not detect any phosphodiesterase activity of GDE5 in the presence of 1 mM $CaCl_2$ (data not shown). Furthermore, to examine the involvement of GDE5 in the hydrolysis of GroPCho in mammalian cells, we used a siRNA-mediated GDE5 knockdown in NIH3T3 cells (supplemental Fig. S3*A*). GDE5 RNAi gene silencing resulted in an increase in intracellular GroPCho levels (supplemental Fig. S3*B*). Taken together, these observations indicated that GDE5 is an UgpQ-type GDE and that GroPCho is a GDE5 substrate.

GDE5 mRNA Expression Is Altered during Skeletal Muscle Atrophy—To evaluate the physiological roles of GDE5, we first characterized the tissue-specific expression of GDE5 mRNA and showed that the transcript is highly expressed in mouse skeletal muscle and cardiac muscle tissues (Fig. 3*A*), thus suggesting a functional role of GDE5 in these muscle tissues. The mass and composition of skeletal muscle, which are critical for its functions, are widely known to be strongly associated with

decreased physical activity. We then investigated whether GDE5 mRNA expression was altered in skeletal muscle under physiological or pathological conditions. GDE5 mRNA expression in skeletal muscle was down-regulated in several types of skeletal muscle atrophies such as aging, denervation, and use of a plaster cast (Fig. 3, *B–D*). Moreover, in diabetic KK-Ay mice, GDE5 mRNA expression appeared to be decreased in skeletal muscle (Fig. 3*E*).

GDE5 Suppresses Myogenic Differentiation—To explore the biological significance of a decrease in GDE5 expression in skeletal muscle, we used siRNA-mediated GDE5 knockdown in C2C12 mouse myoblasts. The amount of reduced RNA and protein expression was assessed by quantitative RT-PCR (Fig. 4, *A* and *B*) and Western blotting (Fig. 4*C*). The extent of differentiation was determined by the fusion index (number of myotubes/total number of nuclei) (Fig. 4, *D* and *E*). GDE5 RNAi gene silencing resulted in strongly enhanced myotube formation during skeletal muscle differentiation, which was accompanied by enhanced expression of myogenin mRNA (Fig. 4, *A* and *B*) and protein (Fig. 4*F*). To examine the inhibitory function of GDE5 during skeletal muscle development, we next investigated whether increased expression of GDE5 would modulate myogenic differentiation. Here, to explore the possibility that GDE5 exerts its biological activity via a non-enzymatic mechanism, we additionally prepared a truncated version (GDE5ΔC471) of mouse GDE5 (Fig. 5*A*). The sequence lacked a C-terminal domain (amino acids 471–675) but retained the GDE sequence identified as a cluster of strictly conserved residues (His-326, Arg-327, Glu-343, Asn-344, Glu-361, His-376, Asp-377, Glu-461, and Lys-463). An enzymatic assay using HEK293T cells overexpressing WT GDE5 (GDE5wt) or GDE5ΔC471 showed that GroPCho can be hydrolyzed by GDE5wt but not by GDE5ΔC471, with no difference in protein stability between the two forms (Fig. 5, *B* and *C*, and supplemental Fig. S4). These data indicated that the GP-PDE conserved cluster sequence was not sufficient for GroPCho phosphodiesterase activity and that GDE5ΔC471 is a useful tool for studying the non-enzymatic function of GDE5 because of the presence of the intact GP-PDE sequence. To examine the effects of increased GDE5 expression on myogenic differentiation, we developed C2C12 myoblasts stably expressing GDE5wt or GDE5ΔC471 and assessed the selected markers of myoblastic differentiation. Forced expression of GDE5wt and GDE5ΔC471 decreased myotube formation (Fig. 5, *D* and *E*) and myogenin mRNA expression levels (Fig. 5, *F* and *G*) compared with the C2C12 control pooled clones. The results indicated that both GDE5wt and GDE5ΔC471 suppressed myogenic differentiation of C2C12 cells.

To further confirm the negative regulation of myogenic differentiation by GDE5wt and GDE5ΔC471, we infected L6 rat skeletal myoblasts with retroviruses harboring GFP, GDE5wt, or GDE5ΔC471 (Fig. 6*A*). At 7 days, WT L6 cells had elongated and begun to align with one another (Fig. 6*B*). In contrast, L6 cells expressing GDE5wt or GDE5ΔC471 were well spread, with no polarization or significant changes in morphology (Fig. 6*B*). We quantified the extent of myogenic differentiation by scoring the appearance of elongated cells (Fig. 6*C*) and muscle-specific mRNA expression such as myogenin and creatine kinase (Fig. 6, *D–F*). Viewed together, these observations indicated that GDE5 can inhibit myogenic differentiation and that this action of GDE5 in skeletal

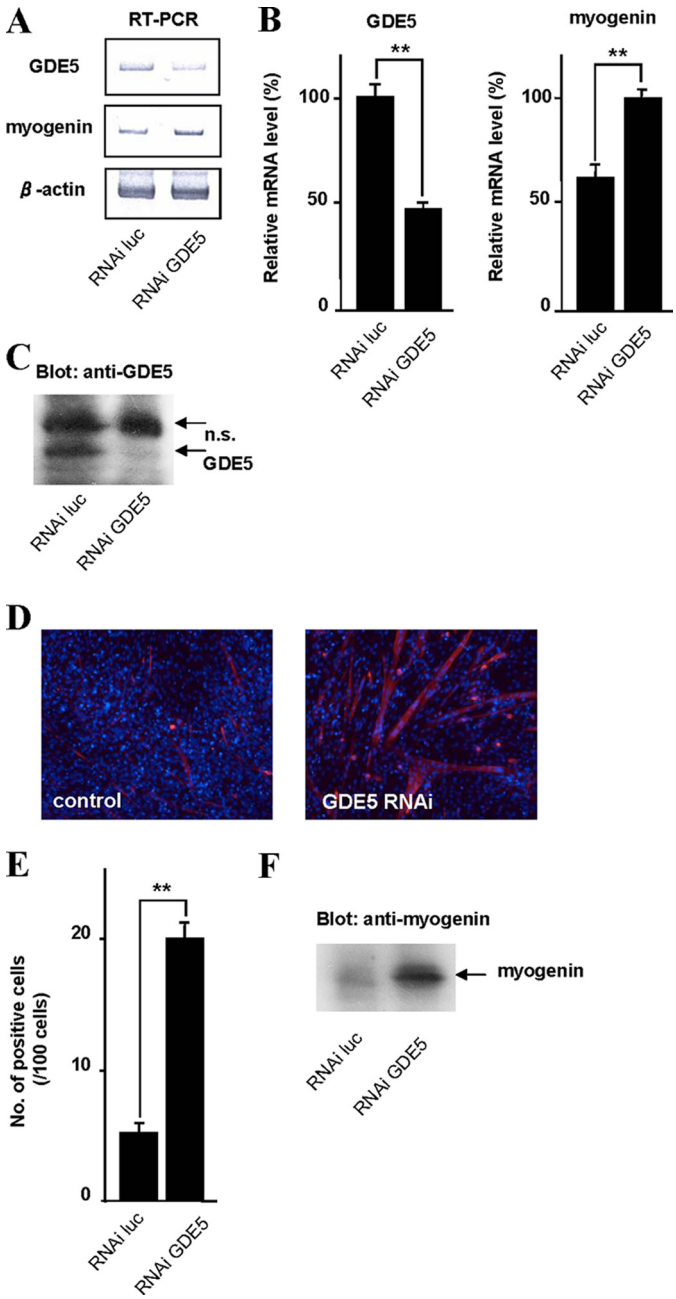

FIGURE 4. **Effects of GDE5 siRNA on C2C12 myogenesis.** C2C12 myoblasts were transfected with luciferase siRNA (*RNAi luc*) or GDE5 siRNA (*RNAi GDE5*). *A* and *B*, after 2 days of transfection (day 0), total RNA was extracted and subjected to RT-PCR (*A*) and quantitative PCR analyses (*B*) to examine expression levels of GDE5 and myogenin mRNAs. The level of β-actin transcript was used as a control. At day 0, whole cell lysates were obtained, and total protein extracts (10 μg/lane) were subjected to SDS-PAGE followed by Western blotting using an anti-GDE5 antibody (*C*) and an anti-myogenin antibody (*F*). *n.s.*, non-specific band. *D*, at day 0, the growth medium was changed to differentiation medium containing 2% horse serum. At day 3, C2C12 cells were fixed and subjected to immunofluorescent staining using a mouse anti-myosin (fast) antibody, which was visualized with a Cy3-conjugated secondary antibody (*red*). Then the nuclei were stained with 4′,6-diamidino-2-phenylindole (*blue*). Magnification, ×100. *E*, the numbers of myotubes (number of myotubes/total number of nuclei) were counted in eight randomly chosen fields in each dish. **, $p < 0.01$ compared with those of cells transfected with control siRNA (RNAi luc). All values are expressed as mean ± S.E. Statistical significance was determined by an unpaired Student's *t* test.

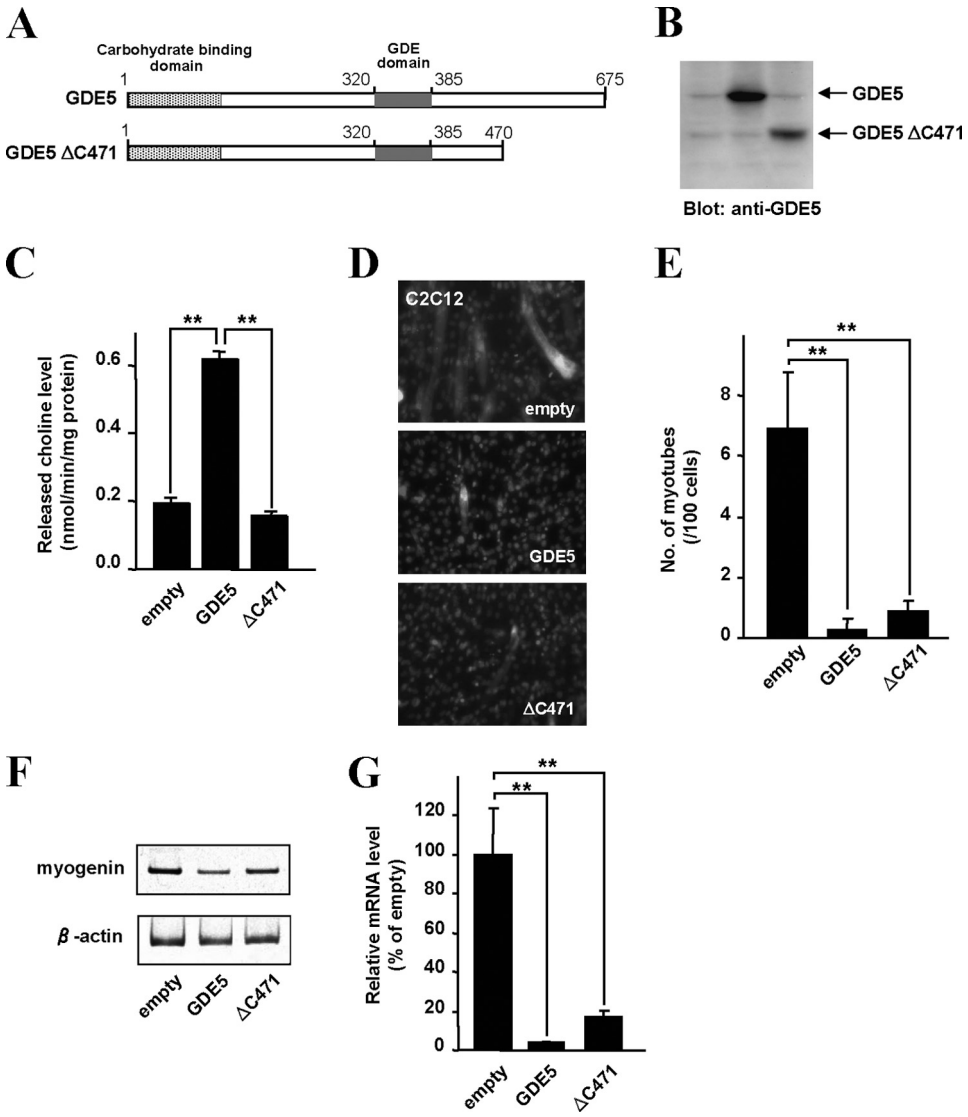

FIGURE 5. **GDE5 suppresses myoblast differentiation.** *A*, schematic diagram of full-length GDE5 and a truncated GDE5 construct (GDE5ΔC471). HEK293T cells were transiently transfected with GDE5 or GDE5ΔC471 cDNA. *B*, total protein extracts (10 μg/lane) from transfected HEK293T cells were subjected to SDS-PAGE followed by Western blotting using an anti-GDE5 antibody. *C*, total protein extracts (2 μg) from transfected HEK293T cells were subjected to an assay for GroPCho phosphodiesterase activity. GroPCho phosphodiesterase activity was examined by measuring released choline in the presence of 1 mM GroPCho. *D–G*, C2C12 myoblasts were stably transfected with GDE5, GDE5ΔC471, or the empty vector (*empty*), and selected markers of myoblast differentiation were assessed at day 7. *D*, C2C12 cells were fixed and stained with a mouse anti-myosin (fast) antibody, which was visualized with fluorescein isothiocyanate-conjugated secondary antibody. Magnification, ×100. Nuclei were stained with 4′,6-diamidino-2-phenylindole. *E*, the numbers of myotubes were counted under ×100 magnification. *F*, total RNA was extracted and subjected to RT-PCR analysis to measure the expression of myogenin mRNA. The level of β-actin transcript was used as a control. *G*, mRNA abundance of myogenin was measured by quantitative RT-PCR. **, $p < 0.01$ compared with those of control C2C12 cells (*empty*).

muscle cells is independent of its GroPCho phosphodiesterase activity.

Transgenic Mice Specifically Overexpressing GDE5ΔC471 in Skeletal Muscle Have Less Type II Fiber-rich Skeletal Muscle Mass—To gain further insight into the potential role of GDE5 in skeletal muscle *in vivo*, focusing on skeletal muscle mass and muscle fiber differentiation via a non-enzymatic mechanism, we established transgenic mice specifically overexpressing GDE5ΔC471 in their skeletal muscle. Here, the human skeletal muscle α-actin promoter was used to control expression of the mouse *GDE5ΔC471* transgene in mice (Fig. 7*A*). During embryonic development, cardiac muscle α-actin is the predominant isoform of sarcomeric α-actin in mice, and the switch to skeletal muscle α-actin occurs postpartum (26). Thus, by using the skeletal muscle α-actin promoter, the possibility that embryonic expression of GDE5ΔC471 might interfere with development was minimized. We obtained two independent lines of transgenic mice (T7 and T31). The *GDE5ΔC471* transgene was evaluated by Northern blotting with RNA isolated from the tissues of GDE5ΔC471 mice and age-matched control mice at 10 weeks of age. Transgene expression was observed not only in the gastrocnemius and quadriceps, but also in other areas of skeletal muscle, including the soleus (Fig. 7*B*), indicating that the use of the skeletal muscle α-actin promoter resulted in high expression levels of the transgene in skeletal muscle tissues. Additionally, we prepared an antibody that recognized the mouse GDE5 protein and confirmed the presence of the GDE5ΔC471 protein in muscle protein lysates obtained from the gastrocnemius (Fig. 7*C*). Body weight and blood metabolite levels (free fatty acids and glucose) were not significantly different between the GDE5ΔC471 mice (both lines) and the control mice (Table 1). However, in GDE5ΔC471 mice (both lines), the skeletal muscle, especially type II fiber-rich muscle, was smaller in size than that of control mice (Fig. 7*D* and Table 2). Moreover, in the skeletal muscle of GDE5ΔC471 mice there were decreases in the expression levels of genes related to structural proteins of type II fibers (fast twitch muscle) such as fast muscle isoforms of troponins (Fig. 7*E*). To better visualize the morphology of the muscle fibers, transverse sections of skeletal muscle (quadriceps) of transgenic and control mice were stained with hematoxylin and eosin, which revealed reduced skeletal muscle mass and smaller fibers in GDE5ΔC471 mice as compared with the controls (Fig. 7*F*). In particular, the mean fiber cross-sectional areas of the GDE5ΔC471 mice were reduced by 55% compared with the controls. Plotting the fiber area as a frequency distribution showed a leftward shift, indicating an evident increase in the percentage of small areas in

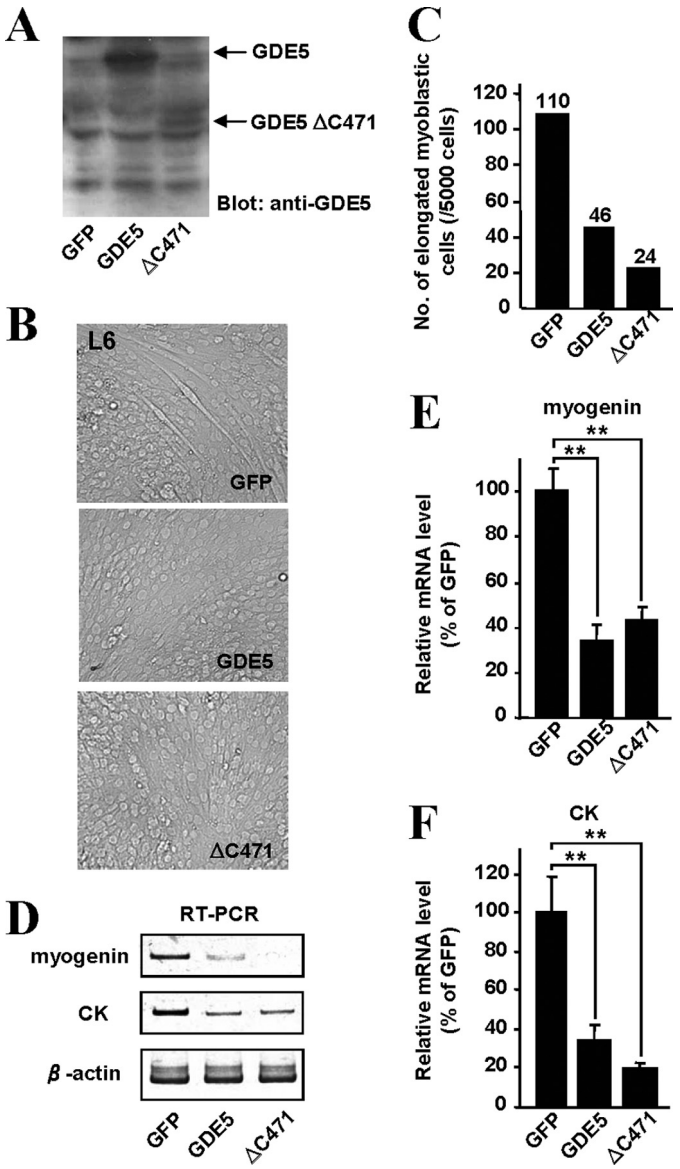

FIGURE 6. **Retroviruses harboring GFP, GDE5, or GDE5ΔC471 were used to infect L6 myoblasts.** *A*, total protein extracts (10 μg/lane) from infected L6 myoblasts were subjected to SDS-PAGE followed by Western blotting using an anti-GDE5 antibody. *B*, the morphology of each cell line cultured in the myogenic medium for 10 days was observed under light microscopy. Magnification, ×100. *C*, to quantitatively evaluate myogenesis, elongated cells (per 5000 cells) were counted in each dish. *D*, total RNA was extracted and subjected to RT-PCR analysis to measure the expression of myogenin and creatine kinase (*CK*) mRNAs. The level of β-actin transcript was used as a control. *E* and *F*, quantitative RT-PCR was performed to estimate the mRNA abundance of myogenin and creatine kinase. **, $p < 0.01$ compared with those of L6 cells infected with GFP. All values are expressed as means ± S.E. Statistical significance was determined by unpaired Student's *t* test.

the GDE5ΔC471 mice (Fig. 7*G*). To examine whether the decreased skeletal muscle mass of the GDE5ΔC471 mice affected their systemic glucose homeostasis, we tested oral glucose tolerance in the GDE5ΔC471 mice after an 8-week, high fat diet containing high amounts of beef tallow. Glucose tolerance, however, did not differ significantly between the GDE5ΔC471 mice and the controls (data not shown). To obtain information on changes in gene expression in the GDE5ΔC471 mice, we performed microarray analysis using RNA samples from the skeletal muscle (quadriceps) of transgenic and control mice. Interestingly, the expression of several genes linked to neuromuscular junctions was up-regulated in the skeletal muscle of the GDE5ΔC471 mice (Table 3). Reverse transcription-polymerase chain reaction assays also showed that mRNA transcripts for nicotinic acetylcholine receptors (α1, γ, and ϵ subunits) and nestin were more abundant in GDE5ΔC471 than in control muscles (Fig. 8). These observations suggested that the compensatory expression of components localized at the neuromuscular junctions in the GDE5ΔC471 skeletal muscle have preventive effects on skeletal muscle dysfunction. As noted also, mRNA expressions of a variety of α-defensins within the antimicrobial peptide family were significantly up-regulated in the skeletal muscle of GDE5ΔC471. α-Defensins are reported to be effectors of mammalian innate immunity; they are found in phagocytic leukocytes of myeloid origin and in the small intestine following secretion by epithelial Paneth cells. Paneth cells have also been shown to secrete α-defensins and additional antimicrobial peptides at high levels in response to cholinergic stimulation (27). Considering that no lymphocytic infiltrate or any other inflammatory signs were present in the skeletal muscle of GDE5ΔC471 (data not shown), up-regulated expression of α-defensins in the muscles may be dependent on activation of the acetylcholine receptor pathway due to the increased levels of neuromuscular junction components.

DISCUSSION

In this study, we have shown that a novel cytosolic GP-PDE, GDE5, selectively hydrolyzes GroPCho. To date, GP-PDEs have been found widely in bacteria, yeast, plants, and mammals. However, different physiological roles among the GP-PDEs have been discussed (10, 22, 28–33). Bacterial GlpQs are well studied and have been shown to have important functions in the hydrolysis of deacylated glycerophospholipids to glycerol phosphate, which is a major source of carbon and phosphate (10, 28). Previous studies have examined several types of glycerophosphodiesters (derived from glycerophospholipids) as substrates for bacteria GP-PDEs and demonstrated that the bacterial enzymes show broad substrate specificities toward glycerophosphodiesters (10, 24, 28), providing an advantage for the acquisition of glycerol 3-phosphate to be metabolized in bacteria. In contrast, an intriguing feature of mammalian GP-PDEs is that these enzymes show restricted substrate specificities, strongly suggesting the physiological roles of mammalian GP-PDEs as a determinant for GroPIns or GroPCho levels in mammalian cells. GroPIns has been shown to be involved in the control of cell proliferation, cell chemotaxis, and cell morphology, affecting in the last case actin cytoskeletal rearrangements through the activation of small GTPases of the Rho family (9, 34, 35), whereas GroPCho is reportedly an osmoprotective compatible and counteracting organic osmolyte that accumulates in renal inner medullary cells in response to high NaCl and urea (8, 36, 37). A recent study suggests that GDE2 contributes to osmotic regulation as a GroPCho phosphodiesterase (38). This study shows that GDE5 can hydrolyze GroPCho preferentially, suggesting that this novel cytosolic GP-PDE has a role in maintaining the intracellular osmotic balance by regulating intracellular GroPCho.

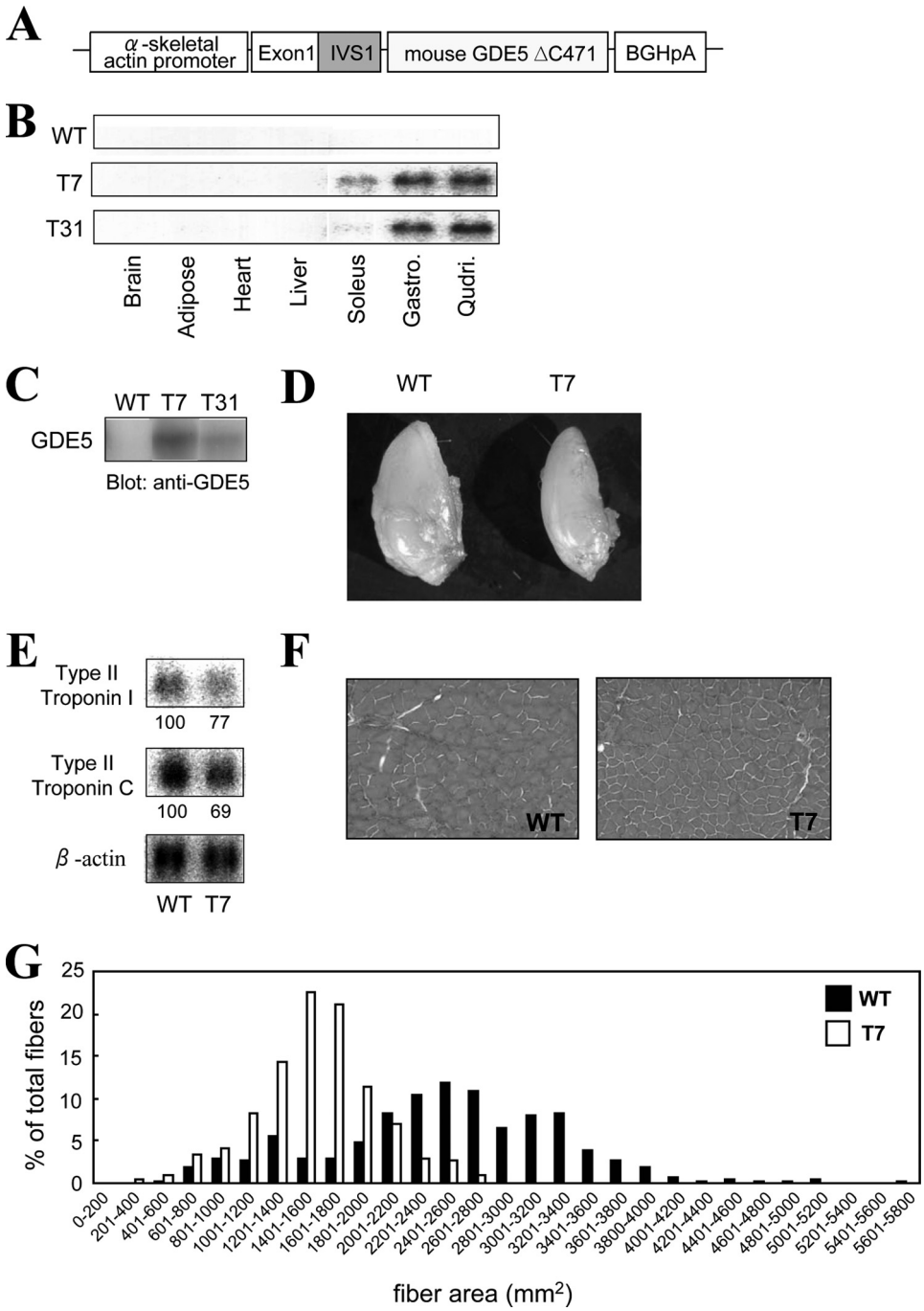

FIGURE 7. **Creation of GDE5ΔC471 transgenic mice.** *A*, map of construct used for transgenic microinjection. The transgene was under the control of the human skeletal muscle α-actin promoter and included exon 1 and the intron of the human skeletal muscle α-actin gene, as well as the bovine growth hormone polyadenylation site. *B*, Northern blotting was performed to examine GDE5ΔC471 mRNA expression in tissues from GDE5ΔC471 mice (cell lines *T7* and *T31*) and non-transgenic control mice (*WT*). Total RNAs from brain, white adipose tissue (*adipose*), heart, kidney, liver, and skeletal muscle (soleus, gastrocnemius (*Gastro.*), and quadriceps (*Quadri.*)) were analyzed using a cDNA probe of bovine growth hormone polyadenylation sequence to detect only GDE5ΔC471 mRNA. Each *lane* contained 10 μg of total RNA. *C*, expression of GDE5ΔC471 in skeletal muscle of GDE5ΔC471 mice. Protein extracts (10 μg/lane) were subjected to SDS-PAGE. GDE5ΔC471 protein was detected by immunoblotting. *D*, comparison of dissected skeletal muscle (gastrocnemius) for 12-week-old GDE5ΔC471 mice (*T7*) and age-matched control mice (*WT*). The muscles were smaller in size in the GDE5ΔC471 mice than in the control mice. *E*, Northern blotting was performed on total RNA (10 μg/lane) isolated from skeletal muscle (quadriceps) of the GDE5ΔC471 mice (*T7*) and non-transgenic control mice (*WT*). cDNA from type II troponin I (fast), type II troponin C (fast), and β-actin was used. *Numbers* below the panels are ratios relative to β-actin (the signal of the control for each sample was set at *100*). *F* and *G*, H&E staining of tissue sections from quadriceps of 12-week-old GDE5ΔC471 mice (*T7*) and age-matched control mice (*WT*). Images were analyzed to quantify the fiber areas.

In the present study, we have demonstrated that GDE5 inhibits skeletal muscle differentiation. It is puzzling that GDE5 mRNA expression in skeletal muscle was down-regulated in several types of skeletal muscle atrophies. As previous studies have suggested functional adaptations of skeletal muscle during denervation, disuse, and aging (39), the decreased GDE5 expression might represent an adaptation response to counteract the pathology. Further, we have shown that the GDE5 inhibitory role is not due to its GroPCho phosphodiesterase activity. Previous studies using yeast two-hybrid systems have shown that mammalian GP-PDEs have the potential to interact with intracellular proteins (12, 20). Yan *et al.* (21) recently described a remarkable characteristic of a mammalian GP-PDE, namely, that GDE2 interacts with the antioxidant scavenger peroxiredoxin1 (Prdx1) and cooperates with Prdx1 to drive neuronal differentiation. These observations suggested that mammalian GP-PDEs coordinate intracellular proteins in the control of cellular events. Further studies, which should include the isolation of molecules that interact with GDE5ΔC471, will be necessary to determine the mechanism of action (and other potential functions) of GDE5.

We created transgenic mice specifically expressing GDE5ΔC471 in skeletal muscle and showed that GDE5ΔC471 mice have less type II fiber-rich muscle mass. Previous animal studies have defined the pattern of transcriptional changes in skeletal muscle in pathological and physiological states. Increased mRNA expression of several genes involved in neuromuscular interactions in GDE5ΔC471 skeletal muscle is similar to the multiple types of skeletal muscle atrophy characterized by structural alterations of the neuromuscular junctions (40, 41). Moreover, as shown in Table 3, it is worth noting that the mRNA expression of genes encoding the polyamine biosynthetic enzymes spermine oxi-

TABLE 1

Body weight, blood glucose, free fatty acid, and triglyceride concentrations of 12-week-old GDE5ΔC471 mice (both line T7 and line T31) and age-matched control mice

Body weight and blood metabolites (glucose, free fatty acid, and triglyceride) levels were not significantly different between GDE5ΔC471 mice (both lines) and control mice.

Mice	Body weight	Glucose	Free fatty acid	Triglyceride
	g	*mg/dl*	*meq/liter*	*mg/dl*
Control	23.8 ± 0.4	161 ± 32	0.24 ± 0.05	63 ± 9
T7	22.4 ± 1.2	165 ± 7	0.23 ± 0.05	65 ± 11
Control	20.5 ± 0.4	162 ± 6	0.33 ± 0.08	69 ± 15
T31	19.8 ± 0.4	170 ± 16	0.37 ± 0.06	73 ± 11

TABLE 2

Wet weights of tissues including skeletal muscles (quadriceps (Quadri.), gastrocnemius (Gastro), and soleus) of 12-week-old GDE5ΔC471 mice (both the T7 and T31 lines) and age-matched control mice

Only skeletal muscles, especially type II fiber-rich muscles, in GDE5ΔC471 mice (both lines) were smaller in size than those of the control mice. Liver, heart, and kidney weights of control and GDE5ΔC471 mice did not differ significantly. Values represent means ± S.E. ($n = 4$).

Mice	Quadri.	Gastro.	Soleus	Liver	Heart	Kidney
	mg	*mg*	*mg*	*mg*	*mg*	*mg*
Control	176 ± 3	135 ± 2	7.9 ± 0.5	0.99 ± 0.05	110 ± 4	143 ± 6
T7	115 ± 7[a]	96 ± 7[a]	6.7 ± 0.2	1.04 ± 0.06	105 ± 5	137 ± 5
Control	155 ± 5	106 ± 5	5.6 ± 0.2	0.79 ± 0.02	98 ± 2	114 ± 6
T31	114 ± 2[a]	93 ± 3[b]	6.1 ± 0.2	0.79 ± 0.03	100 ± 7	124 ± 2

[a] $p < 0.01$.
[b] $p < 0.05$.

dase and *S*-adenosylmethionine decarboxylases was decreased in the GDE5ΔC471 muscle. Previous studies have demonstrated that androgen hormones and/or physical exercise influence polyamine metabolism in skeletal muscle (42, 43). It is thus possible that down-regulation of polyamine synthesis is involved in the pathologic process in GDE5ΔC471 skeletal muscle. In most types of skeletal muscle atrophy, such as disuse and denervation, the overall rates of protein synthesis are suppressed and the rates of protein degradation are consistently elevated; this response accounts for the majority of the rapid loss of muscle protein (44, 45). In animal models (*e.g.* denervation and immobilization), most of the accelerated proteolysis in skeletal muscle appears to be due to an activation of the ubiquitin-proteasome pathway, accompanied by significant increases in mRNA levels of the ubiquitin ligase genes *Atrogin-1/MAFbx*, *MuRF-1*, and *Cbl-b*, which are rate-limiting enzymes in the protein-ubiquitin system (46–48). In GDE5ΔC471 mice, mRNA levels for genes encoding enzymes involved in the ubiquitin-proteasome pathway and certain proteasome subunits did not differ from the controls, suggesting that protein degradation of skeletal muscle is not involved in the pathology of GDE5ΔC471 muscles. Of interest, this *in vivo* study demonstrated that the mRNA expression of a variety of secreted proteins, such as antimicrobial α-defensins and Reg members, is

TABLE 3

GDE5ΔC471 affects the expression of multiple genes in skeletal muscles (quadriceps)

Differentially expressed genes grouped into functional categories are listed. A DNA microarray analysis was repeated with the Cy3 and Cy5 dyes reversed (dye swap). The -fold change (-Fold) represents the average mRNA expression level in GDE5ΔC471 mice (T7 line) relative to control mice.

Gene ID	Gene symbol	Gene description	*p* Value	-Fold
Structural proteins				
AF221104	Kifc5c	Kinesin-related protein KIFC5C	0.00000	10.85
XM_001000857	Tchh	Trichohyalin	0.00000	9.89
NM_031170	Krt8	Keratin 8	0.00018	2.20
NM_010664	Krt18	Keratin 18	0.00000	4.80
NM_001033177	Krt76	Keratin 76	0.00220	4.66
NM_008508	Lor	Loricrin	0.00000	7.32
Secreted proteins				
NM_009043	Reg2	Regenerating islet-derived 2	0.00000	20.56
NM_017399	Fabp1	Fatty acid-binding protein 1, liver	0.00000	24.62
NM_011036	Pap	Pancreatitis-associated protein	0.00000	10.03
NM_026925	Pnlip	Pancreatic lipase	0.00000	15.23
NM_025467	Gkn2	Gastrokine 2	0.00000	23.87
NM_170727	Scgb3a1	Secretoglobin, family 3A, member 1	0.00000	9.42
Neuromuscular junctions				
NM_009599	Ache	Acetylcholinesterase	0.00000	3.96
NM_007389	Chrna1	Nicotinic acetylcholine receptor, α-subunit 1	0.00000	6.30
NM_009604	Chrng	Nicotinic acetylcholine receptor, γ-subunit	0.00000	5.23
NM_009603	Chrne	Nicotinic acetylcholine receptor, ϵ-subunit	0.00000	3.67
NM_016701	Nes	Nestin	0.00000	4.21
NM_010875	Ncam1	Neural cell adhesion molecule 1 (NCAM1)	0.00000	4.06
Channels				
NM_017474	Clca3	Chloride channel calcium-activated 3	0.00000	7.11
NM_021487	Kcne1l	Potassium voltage-gated channel, Isk-related family	0.00000	7.45
NM_010597	Kcnab1	Potassium voltage-gated channel, shaker-related subfamily, β1	0.00000	−3.82
Cell defense and stress response				
NM_001012307	Defcr23	Defensin-related cryptdin 23	0.00000	21.93
NM_010031	Defa1	Defensin, a1	0.00000	21.88
NM_007852	Defcr6	Defensin-related cryptdin 6	0.00000	29.56
NM_007847	Defcr-rs2	Defensin-related cryptdin, related sequence 2	0.00000	7.37
NM_008181	Gsta1	Glutathione *S*-transferase, α1 (Ya)	0.00000	8.28
NM_008182	Gsta2	Glutathione *S*-transferase, α2 (Yc2)	0.00000	8.10
NM_008361	Il1b	Interleukin 1β	0.00010	4.31
Amino acid metabolism and polyamine synthesis				
NM_009665	Amd1	*S*-Adenosylmethionine decarboxylase 1	0.00000	−5.02
NM_007444	Amd2	*S*-Adenosylmethionine decarboxylase 2	0.00000	−3.61
NM_009414	Tph1	Tryptophan hydroxylase 1	0.00000	−4.10
NM_145533	Smox	Spermine oxidase	0.00000	−3.29

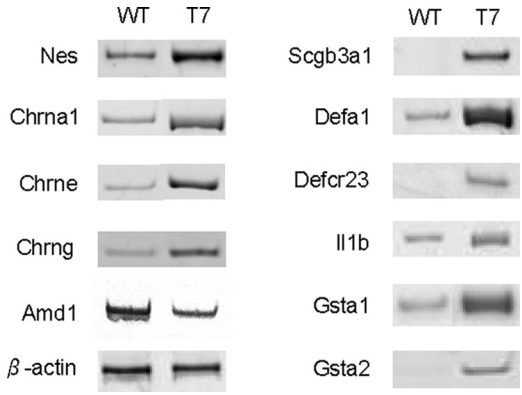

FIGURE 8. **GDE5ΔC471 affects the expression of multiple genes in skeletal muscle (quadriceps).** Semiquantitative RT-PCR was performed to determine the mRNA levels of selected genes from Table 3.

up-regulated in GDE5ΔC471 muscle. Recent studies have demonstrated novel biological roles of α-defensins in fibroblast proliferation and collagen synthesis, via the β-catenin signaling pathway, and in the suppression of hepatic glucose production, through a mechanism distinct from the classical insulin signaling pathway (49, 50). As noted also, we have shown that white adipose tissue weights of 1-year-old GDE5ΔC471 mice were increased as compared with age-matched controls (supplemental Table S1), suggesting that the secreted proteins from skeletal muscle of the GDE5ΔC471 mice can modulate white adipose tissue functions and mass with aging. Furthermore, Livesey *et al.* (51) showed that Reg2 (regenerating islet-derived 2) is a potent Schwann cell mitogen involved in motor neuron regeneration and development. Thus, GDE5ΔC471 mice not only will contribute to an understanding of the *in vivo* functions of GDE5 via a non-enzymatic mechanism, but they will also be available as a novel animal model of type II fiber-rich skeletal muscle diseases that can be used to screen for new myokines in skeletal muscles.

In summary, this study provides a new insight into the role of mammalian GP-PDEs, independent of their enzymatic activity. It also has prompted us to further consider the evolutionary differences between and biological significance of prokaryotic and mammalian GP-PDEs at the molecular level.

Acknowledgment—We thank Cristiano Iurisci for technical assistance.

REFERENCES

1. Zurlo, F., Larson, K., Bogardus, C., and Ravussin, E. (1990) *J. Clin. Investig.* **86,** 1423–1427
2. Berchtold, M. W., Brinkmeier, H., and Müntener, M. (2000) *Physiol. Rev.* **80,** 1215–1265
3. Proctor D. N, Balagopal P, and Nair K. S (1998) *J. Nutr.* **128,** (suppl.) S351–S355
4. Burt, C. T., Glonek, T., and Bárány, M. (1976) *Biochemistry* **15,** 4850–4853
5. Younkin, D. P., Berman, P., Sladky, J., Chee, C., Bank, W., and Chance, B. (1987) *Neurology* **37,** 165–169
6. Sprott, H., Rzanny, R., Reichenbach, J. R., Kaiser, W. A., Hein, G., and Stein, G. (2000) *Rheumatology* **39,** 1121–1125
7. Baburina, I., and Jackowski, S. (1999) *J. Biol. Chem.* **274,** 9400–9408
8. Gallazzini, M., and Burg, M. B. (2009) *Physiology* **24,** 245–249
9. Corda, D., Zizza, P., Varone, A., Filippi, B. M., and Mariggiò, S. (2009) *Cell. Mol. Life Sci.* **66,** 3449–3467
10. Larson, T. J., Ehrmann, M., and Boos, W. (1983) *J. Biol. Chem.* **258,** 5428–5432
11. Tommassen, J., Eiglmeier, K., Cole, S. T., Overduin, P., Larson, T. J., and Boos, W. (1991) *Mol Gen Genet.* **226,** 321–327
12. Zheng, B., Chen, D., and Farquhar, M. G. (2000) *Proc. Natl. Acad. Sci. U.S.A.* **97,** 3999–4004
13. Yanaka, N., Imai, Y., Kawai, E., Akatsuka, H., Wakimoto, K., Nogusa, Y., Kato, N., Chiba, H., Kotani, E., Omori, K., and Sakurai, N. (2003) *J. Biol. Chem.* **278,** 43595–43602
14. Nogusa, Y., Fujioka, Y., Komatsu, R., Kato, N., and Yanaka, N. (2004) *Gene* **337,** 173–179
15. Rao, M., and Sockanathan, S. (2005) *Science* **309,** 2212–2215
16. Zheng, B., Berrie, C. P., Corda, D., and Farquhar, M. G. (2003) *Proc. Natl. Acad. Sci. U.S.A.* **100,** 1745–1750
17. Yanaka, Y., Nogusa, N., Fujioka, Y., Yamashita, Y., and Kato, N. (2007) *FEBS Lett.* **581,** 712–718
18. Corda, D., Kudo, T., Zizza, P., Iurisci, C., Kawai, E., Kato, N., Yanaka, N., and Mariggiò, S. (2009) *J. Biol. Chem.* **284,** 24848–24856
19. Corda, D., Iurisci, C., and Berrie, C. P. (2002) *Biochim. Biophys. Acta.* **1582,** 52–69
20. Bachmann, A. S., Duennebier, F. F., and Mocz, G. (2006) *Gene* **371,** 144–153
21. Yan, Y., Sabharwal, P., Rao, M., and Sockanathan, S. (2009) *Cell* **138,** 1209–1221
22. Yanaka, N. (2007) *Biosci. Biotechnol. Biochem.* **71,** 1811–1818
23. Okazaki, Y., Furuno, M., Kasukawa, T., Adachi, J., Bono, H., Kondo, S., Nikaido, I., Osato, N., Saito, R., Suzuki, H., Yamanaka, I., Kiyosawa, H., Yagi, K., Tomaru, Y., Hasegawa, Y., Nogami, A., Schönbach, C., Gojobori, T., Baldarelli, R., Hill, D. P., Bult, C., Hume, D. A., Quackenbush, J., Schriml, L. M., Kanapin, A., Matsuda, H., Batalov, S., Beisel, K. W., Blake, J. A., Bradt, D., Brusic, V., Chothia, C., Corbani, L. E., Cousins, S., Dalla, E., Dragani, T. A., Fletcher, C. F., Forrest, A., Frazer, K. S., Gaasterland, T., Gariboldi, M., Gissi, C., Godzik, A., Gough, J., Grimmond, S., Gustincich, S., Hirokawa, N., Jackson, I. J., Jarvis, E. D., Kanai, A., Kawaji, H., Kawasawa, Y., Kedzierski, R. M., King, B. L., Konagaya, A., Kurochkin, I. V., Lee, Y., Lenhard, B., Lyons, P. A., Maglott, D. R., Maltais, L., Marchionni, L., McKenzie, L., Miki, H., Nagashima, T., Numata, K., Okido, T., Pavan, W. J., Pertea, G., Pesole, G., Petrovsky, N., Pillai, R., Pontius, J. U., Qi, D., Ramachandran, S., Ravasi, T., Reed, J. C., Reed, D. J., Reid, J., Ring, B. Z., Ringwald, M., Sandelin, A., Schneider, C., Semple, C. A., Setou, M., Shimada, K., Sultana, R., Takenaka, Y., Taylor, M. S., Teasdale, R. D., Tomita, M., Verardo, R., Wagner, L., Wahlestedt, C., Wang, Y., Watanabe, Y., Wells, C., Wilming, L. G., Wynshaw-Boris, A., Yanagisawa, M., Yang, I., Yang, L., Yuan, Z., Zavolan, M., Zhu, Y., Zimmer, A., Carninci, P., Hayatsu, N., Hirozane-Kishikawa, T., Konno, H., Nakamura, M., Sakazume, N., Sato, K., Shiraki, T., Waki, K., Kawai, J., Aizawa, K., Arakawa, T., Fukuda, S., Hara, A., Hashizume, W., Imotani, K., Ishii, Y., Itoh, M., Kagawa, I., Miyazaki, A., Sakai, K., Sasaki, D., Shibata, K., Shinagawa, A., Yasunishi, A., Yoshino, M., Waterston, R., Lander, E. S., Rogers, J., Birney, E., and Hayashizaki, Y. (2002) *Nature* **420,** 563–573
24. Ohshima, N., Yamashita, S., Takahashi, N., Kuroishi, C., Shiro, Y., and Takio, K. (2008) *J Bacteriol.* **190,** 1219–1223
25. Kates, M. (1972) in *Laboratory Techniques in Biochemistry and Molecular Biology* (Work, T. S., and Work, E., eds) Vol. 3, pp. 347–392, Elsevier Science Publishers B.V., Amsterdam
26. Brennan, K. J., and Hardeman, E. C. (1993) *J. Biol. Chem.* **268,** 719–725
27. Ayabe, T., Satchell, D. P., Wilson, C. L., Parks, W. C., Selsted, M. E., and Ouellette, A. J. (2000) *Nat. Immunol.* **1,** 113–118
28. Larson, T. J., and van Loo-Bhattacharya, A. T. (1988) *Arch. Biochem. Biophys.* **260,** 577–584
29. Fan, X., Goldfine, H., Lysenko, E., and Weiser, J. N. (2001) *Mol. Microbiol.* **41,** 1029–1036
30. van der Rest, B., Boisson, A. M., Gout, E., Bligny, R., and Douce, R. (2002) *Plant Physiol.* **130,** 244–255
31. van der Rest, B., Rolland, N., Boisson, A. M., Ferro, M., Bligny, R., and Douce, R. (2004) *Biochem. J.* **379,** 601–607

32. Fisher, E., Almaguer, C., Holic, R., Griac, P., and Patton-Vogt, J. (2005) *J. Biol. Chem.* **280,** 36110–36117
33. Fernández-Murray, J. P., and McMaster, C. R. (2005) *J. Biol. Chem.* **280,** 38290–38296
34. Mancini, R., Piccolo, E., Mariggiò, S., Filippi, B. M., Iurisci, C., Pertile, P., Berrie, C. P., and Corda, D. (2003) *Mol. Biol. Cell.* **14,** 503–515
35. Filippi, B. M., Mariggiò, S., Pulvirenti, T., and Corda, D. (2008) *Biochim. Biophys. Acta* **1783,** 2311–2322
36. Burg, M. B. (1995) *Am. J. Physiol. Renal Physiol.* **268,** F983–F996
37. Gallazzini, M., Ferraris, J. D., Kunin, M., Morris, R. G., and Burg, M. B. (2006) *Proc. Natl. Acad. Sci. U.S.A.* **103,** 15260–15265
38. Gallazzini, M., Ferraris, J. D., and Burg, M. B. (2008) *Proc. Natl. Acad. Sci. U.S.A.* **105,** 11026–11031
39. Evans, W. J. (2010) *Am J. Clin. Nutr.* **91,** 1123S-1127S
40. Kang, H., Tian, L., Son, Y. J., Zuo, Y., Procaccino, D., Love, F., Hayworth, C., Trachtenberg, J., Mikesh, M., Sutton, L., Ponomareva, O., Mignone, J., Enikolopov, G., Rimer, M., and Thompson, W. (2007) *J. Neurosci.* **27,** 5948–5957
41. Ghedini, P. C., Viel, T. A., Honda, L., Avellar, M. C., Godinho, R. O., Lima-Landman, M. T., Lapa, A. J., and Souccar, C. (2008) *Muscle Nerve* **38,** 1585–1594
42. Turchanowa, L., Rogozkin, V. A., Milovic, V., Feldkoren, B. I., Caspary, W. F., and Stein, J. (2000) *Eur. J. Clin. Invest.* **30,** 72–78
43. MacLean, H. E., Chiu, W. S., Notini, A. J., Axell, A. M., Davey, R. A., McManus, J. F., Ma, C., Plant, D. R., Lynch, G. S., and Zajac, J. D. (2008) *FASEB J.* **22,** 2676–2689
44. Glass, D. J. (2003) *Trends Mol. Med.* **9,** 344–350
45. Jackman, R. W., and Kandarian, S. C. (2004) *Am. J. Physiol. Cell Physiol.* **287,** C834–C843
46. Lecker, S. H., Jagoe, R. T., Gilbert, A., Gomes, M., Baracos, V., Bailey, J., Price, S. R., Mitch, W. E., and Goldberg, A. L. (2004) *FASEB J.* **18,** 39–51
47. Nikawa, T., Ishidoh, K., Hirasaka, K., Ishihara, I., Ikemoto, M., Kano, M., Kominami, E., Nonaka, I., Ogawa, T., Adams, G. R., Baldwin, K. M., Yasui, N., Kishi, K., and Takeda, S. (2004) *FASEB J.* **18,** 522–524
48. Kamei, Y., Miura, S., Suzuki, M., Kai, Y., Mizukami, J., Taniguchi, T., Mochida, K., Hata, T., Matsuda, J., Aburatani, H., Nishino, I., and Ezaki, O. (2004) *J. Biol. Chem.* **279,** 41114–41123
49. Liu, H. Y., Collins, Q. F., Moukdar, F., Zhuo, D., Han, J., Hong, T., Collins, S., and Cao, W. (2008) *J. Biol. Chem.* **283,** 12056–12063
50. Han, W., Wang, W., Mohammed, K. A., and Su, Y. (2009) *FEBS J.* **276,** 6603–6614
51. Livesey, F. J., O'Brien, J. A., Li, M., Smith, A. G., Murphy, L. J., and Hunt, S. P. (1997) *Nature* **390,** 614–618